Hydrogen-induced buckling of Mo(110) at submonolayer coverage

1997 J. Phys.: Condens. Matter 9 6481

(http://iopscience.iop.org/0953-8984/9/31/003)

J. Phys.: Condens. Matter **9** (1997) 6481–6491. Printed in the UK PII: S0953-8984(97)81684-0

Hydrogen-induced buckling of Mo(110) at submonolayer coverage

M Arnold, S Sologub†, W Frie, L Hammer and K Heinz

Lehrstuhl für Festkörperphysik, Universität Erlangen–Nürnberg, Staudtstrasse 7, D-91 058 Erlangen, Germany

Received 7 February 1997

Abstract. The adsorption phase Mo(110)–(2×2)2H is structurally analysed by means of low-energy electron diffraction (LEED). A close theory–experiment fit (Pendry R-factor $R = 0.16$) allows the determination of both a near-threefold-coordinated adsorption site and the detailed reconstructive atomic movements induced in the substrate. The latter are rather complex: in the top Mo layer, hydrogen-coordinated atoms are pulled out of the surface with respect to uncoordinated atoms, leading to a total layer buckling amplitude of 0.06 Å. The second substrate layer is also buckled (0.03 Å) with, however, the Mo atoms below the hydrogen atoms pushed into the surface. The first two interlayer distances relax in the direction of the bulk-like-terminated substrate, as frequently observed for hydrogen-covered surfaces. Yet, compared to the case for Fe(110)–(2×2)2H, the induced buckling of top-layer substrate atoms is different in sign (though similar in magnitude), in spite of practically the same adsorption site being obtained, the structural symmetry of the substrate being the same, and the same sign of work-function change being involved. This indicates a delicate balance between structural and electronic material-specific properties.

1. Introduction

It is well known that hydrogen induces reconstructive movements of substrate atoms when adsorbed on metallic surfaces. Though the reconstructions can be substantial, with even complete atomic rows removed (*missing-row reconstruction*), as observed in a few cases, the atomic displacements are not usually larger than 0.1 Å (for recent reviews, see references [1, 2]). This is interesting from the surface crystallographic point of view, but also for a quantitative understanding of the modified electronic properties, such as the work-function change involved. Yet, most of the existing structural investigations of hydrogen adsorption on metals concentrate on fcc substrates and, according to the newest version of the *Surface Structure Database* [3], only comparatively little quantitative work has dealt with bcc-type substrates [4–13]. Furthermore, in some of these few cases the hydrogen site could not be detected [7, 8, 10], or the adatoms were found to be disordered [6]. In other cases the adsorption was at full coverage without any substrate reconstruction involved [4, 11, 12, 13], or a possible substrate reconstruction was not considered [5]. So, to date, the only hydrogen adsorption phase with both the adsorption site and the substrate reconstruction quantitatively known is that of Fe(110)–(2×2)2H [9]. There, hydrogen was found to reside in twofold-to-threefold-coordinated sites pushing coordinated iron atoms

† On leave from: Institute of Physics, National Ukrainian Academy of Science, Kiev, Ukraine.

0953-8984/97/316481+11$19.50

into the surface and thus producing a buckled surface. Independent measurements disclosed an accompanying decrease of the work function [14, 15].

In the present work, we present a quantitative structure determination of Mo(110)–(2×2)2H, which is very similar to the above-mentioned phase of H/Fe. This is the case as regards the structural symmetry of both the substrate and the adsorbate and—as it will turn out—also as regards the hydrogen adsorption site. Yet, surprisingly, we will see that, in spite of these similarities, the buckling induced on the Mo substrate is different—even in sign—to that induced on Fe. Moreover, the present work completes our earlier investigations of the clean and fully hydrogen covered surfaces of Mo(110) [12]. In the latter case, hydrogen was found to reside in threefold-coordinated sites, i.e. to be coordinated to *all* of the surface atoms. As a consequence, the contraction of the first-interlayer distance (4.0% for the clean surface) is reduced to half its value. Therefore, in the submonolayer regime with only a proportion of the surface atoms being hydrogen coordinated, we expect hydrogen to induce a local buckling of at least the top substrate layer. This holds in particular for the (2×2)2H phase, which, according to the literature [16], and consistently with our work, is the only ordered phase of hydrogen on Mo(110) in the submonolayer regime (coverage $\Theta = 0.5$ ML).

We apply low-energy electron diffraction (LEED) to obtain the adsorption structure of Mo(110)–(2×2)2H. As this should include the hydrogen adsorption site as well as the expected induced substrate reconstruction, considerable demands are put on both the measurement of the intensities and their full dynamical analysis. If the substrate is induced to reconstruct, the intensities of the extra spots might be dominated by this reconstruction rather than by the mere hydrogen scattering. So, the measurement must be precise enough to safely record this hydrogen contribution, which is essential to detecting the adsorption site. Qualitatively, the same holds for the theory side: the theory–experiment fit to be achieved for the rather complex structure expected must be good enough to make it sensitive to the hydrogen scattering which otherwise could remain hidden in some (wrong) displacement of substrate atoms.

The paper is organized as follows. The second section gives details of the sample preparation and intensity measurement. This is followed by a description of the intensity calculations, as well as of the strategy and course of the structure determination. The final section summarizes the structural results, and presents a discussion.

2. Experimental details

The experiments were performed in the same ultra-high-vacuum chamber (base pressure: below 5×10^{-11} mbar) as our earlier investigations of clean and hydrogen-saturated surfaces [12]. A four-grid rear-view LEED optics allowed for both intensity measurements and—used in the retarding-field mode—Auger electron spectroscopy (AES). The sample could be heated up to 2500 K by electron bombardment from the rear, and cooled down to below 100 K by means of direct contact to a liquid nitrogen reservoir. The temperature was measured using a $WRe_{3\%}$–$WRe_{25\%}$ thermocouple directly attached to the sample. Precise adjustment of the crystal orientation in order to ensure normal incidence of the primary electron beam was made possible by the linear and rotational degrees of freedom of the sample manipulator.

In order to exhaust the bulk carbon impurities, the crystal was heated to 1400 K in an oxygen ambient of 2×10^{-7} mbar for ten hours. The remaining oxygen was removed by a flash to 2400 K for 10 minutes. After this treatment, no traces of contamination were observable either in the LEED pattern or by means of AES. After thorough cleaning and

during the measurements, short flashes to 2400 K turned out to be sufficient to remove residual gas contaminations and to restore the clean surface, as was checked by AES. Hydrogen was adsorbed immediately after cooling to below 100 K with a partial pressure of about 10^{-8} mbar. As the $p(2 \times 2)$ structure is the only ordered phase in the intermediate-hydrogen-coverage regime, the optimally ordered phase could be prepared by monitoring the intensity of half-order spots during hydrogen adsorption until a maximum was achieved.

LEED intensity curves were measured at 90 K and for normal incidence of the primary beam, using a computer-controlled video technique as described in detail earlier [17–19]. For the intensity measurement, four video half-frames were averaged to improve the signal-to-noise ratio. This leads to an effective speed of measurement of 80 ms per energy point and beam, which is sufficient to keep the residual gas adsorption below the detection level. As the measurement was at normal incidence, the quality of the spectra could be further enhanced by averaging data for symmetrically equivalent beams. The primary beam intensity was taken in parallel and used for normalization of the spectra. Residual noise was removed by final three-point smoothing. The final data-base as input to the intensity analysis consists of $I(E)$ curves of 12 symmetrically inequivalent beams measured between 50 and 500 eV in steps of 0.5 eV, with a total energy width of $\Delta E = 3150$ eV, of which 2020 eV refer to seven integer-order beams and 1130 eV to five half-order beams.

3. The strategy and course of the intensity analysis

Standard full dynamical computer programs [20] were used for the calculation of the $I(E)$ spectra. The atomic scattering was described by a total of 13 relativistically calculated and spin-averaged phase shifts, which were corrected for thermal vibrations using a bulk Debye temperature of $\Theta_{\mathrm{Mo}} = 450$ K for molybdenum [21] in the subsurface layers, and an adjustable value for the top layer. Hydrogen was assumed to adopt the vibrational amplitude of the substrate, as had proven to be successful in earlier analyses of hydrogen adsorbate systems [9, 22]. Scattering within the atomic layers was calculated by the matrix-inversion method [20], and the layers were stacked using the layer-doubling scheme [23]. Electron attenuation was simulated by a constant imaginary part $V_{0\mathrm{i}} = 6.0$ eV of the inner potential. The real part of the latter was found to be energy dependent, proportional to $1/E$, in accordance with earlier results [24].

For the quantitative comparison of experimental and calculated data, the Pendry R-factor [25] was applied, and its variance was used to estimate the limits of error for the parameters varied. As this R-factor uses the logarithmic derivatives of the intensities with respect to the energy rather than the intensities themselves, it is not sensitive to either the absolute level of the intensities or the intensity relations between different beams. This is unfavourable as regards the determination of an adsorbate-induced substrate reconstruction: the more pronounced this reconstruction is, the higher will be the (energy-averaged) intensity level of the fractional-order beams. As this structural information is lost when using an R-factor that is not sensitive to absolute intensities, it is advisable to use—additionally to the Pendry R-factor—this intensity level as a further and independent guide for the retrieval of the correct structure. Yet, as measured and calculated intensities are never at the same level because of, for example, unavoidable surface roughness, it is more appropriate to use a normalized quantity rather than the absolute level. We therefore use the ratio of average fractional- and integer-order beam intensities, $r = \langle I_f \rangle / \langle I_i \rangle$, as the quantity which should

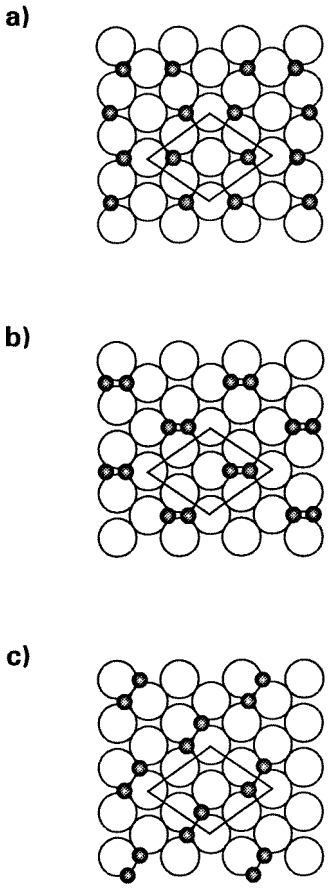

Figure 1. Possible adsorption structures for 0.5 ML hydrogen on Mo(110), assuming threefold-coordinated sites for the adatoms, which yield a p(2 × 2) structure.

be reproduced by intensities calculated for the best-fit model. Hereby,

$$\langle I \rangle = \frac{1}{\Delta E} \int I(E)\ \mathrm{d}E$$

is the energy-averaged and normalized intensity of the group of beams involved. As will be shown below, it may even be reasonable to use the ratio calculated for certain subsets of fractional-order beams.

The first guidance as regards finding the correct structural model comes in fact from the ratio r. It appears that the experimental value calculated for the total of fractional-order beams (index t) is $r_{\mathrm{t}}^{\mathrm{exp}} = 7.3\%$. This is far too high to stem from mere hydrogen scattering, which would produce values in the 1–3% region. So, the value $r_{\mathrm{t}}^{\mathrm{exp}} = 7.3\%$ is a clear indication of some induced substrate reconstruction. However, with the fractional beam intensities being more than an order of magnitude weaker than the substrate intensities, the reconstruction must be rather weak, a conclusion which is in agreement with an R-factor level $R = 0.22$ between the experimental integer-order beams of the (2×2)–2H surface to the intensity of those of the clean surface.

Inspection of the ratio r calculated for different subsets of fractional-order beams yields even more information, in particular regarding the symmetry of the substrate reconstruction involved. Surprisingly, beams with both indices of half-integer order, which we will call *centred* beams (index c) in the following, are considerably more intense on average

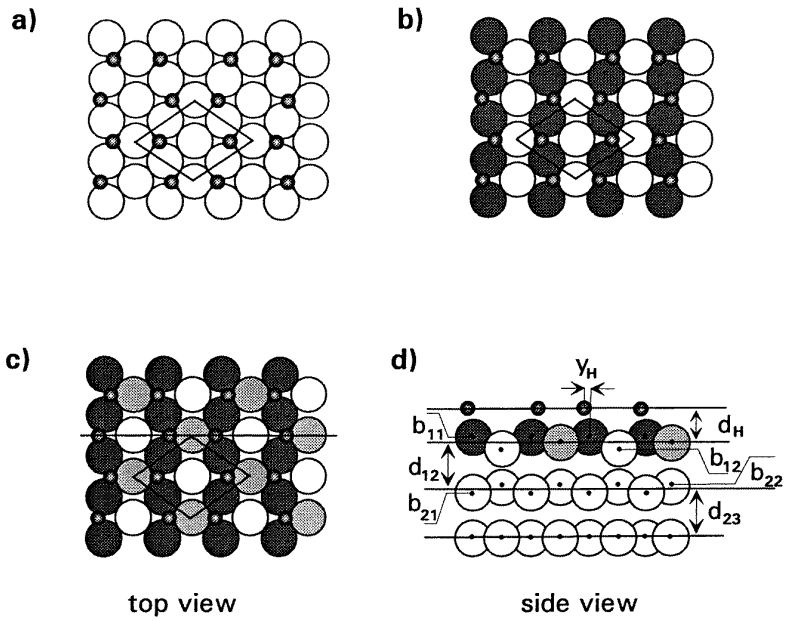

Figure 2. Top: top views of hydrogen adsorbed in threefold-coordinated hollow sites without (a) and with (b) a c(2 × 2) symmetry buckling reconstruction of the substrate. Bottom: a top view (c) and a side view (d) of the best-fit model of Mo(110)–(2 × 2)2H.

than the other (*non-centred*, index nc) beams with only one index being of half-integer order. Quantitatively, this is expressed by the ratios $r_c^{exp} = 9.9\%$ and $r_{nc}^{exp} = 3.5\%$, respectively. Consistently, one observes visually that the centred spots keep their relatively bright intensities up to high energies, in contrast to the behaviour of non-centred spots which are measurable only below 300 eV. This suggests that the main induced substrate reconstruction is of c(2 × 2) symmetry. Some weaker reconstruction with (2 × 2) symmetry and contributions from hydrogen should account for the weaker non-centred spots.

The existence of the two subsets of superstructure spots with different intensity levels described was found to be characteristic also for the Fe(110)–(2 × 2)2H phase [26]. There, adsorbed hydrogen was observed to form a honeycomb-like adlayer, occupying positions close to the threefold-coordinated sites, as shown in model 1 of figure 1(a). Applying quantitative LEED, the threefold-coordinated site was also found for the hydrogen-saturated Mo(110)–(1 × 1)H phase [12]. This is in agreement with findings from density functional theory [27, 28], and is consistent with results from recent highly resolved electron energy-loss spectroscopy (HREELS) measurements [29]. Additionally, in the latter work, only a small shift of the loss peaks was observed when the coverage was increased from 0.4 to 1.0. This indicates that, independently of the coverage, there is only a single adsorption site, and that the local adsorption geometry is only weakly modified with varying coverage. Obviously, a weak H–H interaction allows hydrogen to reside in the locally most favourable site, i.e. the threefold-coordinated site, independently of the coverage. This rules out on-top and bridge sites. Also, combinations of threefold-coordinated sites, as indicated by the remaining models given in figure 1, are highly unlikely, because the adatoms in these models reside closer to each other than is physically reasonable (other combinations of threefold-coordinated sites lead to (2 × 1) or c(2 × 2) structures).

We therefore started with the honeycomb adsorption model (model 1 in figure 1(a), repeated as figure 2(a)) as the most promising trial structure. As expected, there was no good fit to experimental data without any substrate reconstruction considered, either as regards the R-factor ($R = 0.54$), or as regards the intensity level of the fractional-order beams ($r = 0.7\%$). Guided by the experimental findings, we followed a strategy which first determines the most influential structural parameters, and then addresses more and more detailed refinements. The latter include also the precise adatom position, which can only be reliably determined when the substrate structure is already broadly known.

As described above, the most prominent feature of the adsorbate reconstruction is its dominating c(2×2) symmetry. Inspection of the honeycomb model (figure 2(a)) tells us that such a reconstruction develops when in the top substrate layer every second atomic row in the [001] direction is displaced—for example, vertically to the surface, as indicated by the hatched atoms in figure 2(b). In fact, these rows are different from their neighbouring rows—namely, by virtue of the fact that *all* of their atoms (rather than only every second one) are hydrogen coordinated. Therefore, as a first step, we modelled the c(2×2) reconstruction by assuming that full coordination with hydrogen atoms will lead to a layer buckling in the $[\bar{1}10]$ direction caused by the respective atoms being either pulled out of the surface, as found for H/Ni(111), or pushed into it, as is known to occur for H/Fe(110) [9]. This creates two sublayers of c(2×2) symmetry. In this first step, the adsorbate atom was kept fixed at the ideally threefold-coordinated site, with only the height above the substrate simultaneously adjusted. As no pronounced multilayer relaxation can be expected for a (nearly) close-packed surface, as confirmed also for clean Mo(110) [12], only the first three interlayer distances $d_{i,i+1}$ ($i = 1, 2, 3$) were varied, in addition to the intralayer buckling amplitude.

As a result, and similarly to the case for the above-mentioned system H/Fe, two minima develop as a function of the buckling amplitude, as displayed in figure 3, with all of the interlayer distances optimized at each point. The minimum which develops for pulling the hydrogen-coordinated rows of the molybdenum atoms out of the surface is more pronounced (positive buckling amplitude, $R = 0.35$) than the one appearing for the reconstruction in the opposite direction, i.e. for the H-coordinated atoms being pushed into the crystal (negative buckling amplitude, $R = 0.42$). As the R-factor difference is not significant enough to favour one of the two reconstructions, we considered both of them in the following process of structural refinement. The latter included a similar reconstruction in the second layer, and an additional reconstruction of (2×2) symmetry in the top layer. In the course of that refinement, in particular the theory–experiment fit for the fractional-order beams could not be substantially improved for the reconstruction with positive buckling, i.e. the related R-factor for just the fractional-order beams did not drop below $R_{\mathrm{f}} = 0.49$ (corresponding to $R = 0.25$ for the total of the beams). Therefore, the further presentation of results can be limited to the refinement of the minimum with positive buckling, i.e. H-coordinated atoms pulled out of the surface.

Taking again the example of the H/Fe system, a buckling of the second substrate layer was introduced whereby molybdenum atoms below hydrogen atoms were either pushed into the surface or pulled out. (By symmetry arguments, the second-layer reconstruction must be of the c(2×2) type.) Only for the displacement into the surface does the R-factor for the fractional-order spots improve from $R_{\mathrm{f}} = 0.62$ to $R_{\mathrm{f}} = 0.42$, i.e. the displacements of the Mo atoms near hydrogen in the first and second layers are different in sign. Yet, the decrease of R_{f} is only due to the improvement of the centred-spot intensities, as is easily understandable from the fact that up to now, in both the first and the second layer, only reconstructions of c(2×2) symmetry were considered. For the non-centred spots, both the intensity level and

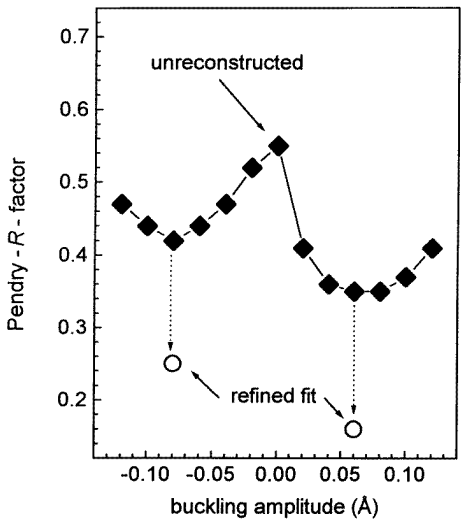

Figure 3. The *R*-factor dependence for Mo(110)–(2×2)2H on the buckling in the top layer according to the atomic displacements as indicated in figure 2(b). The open circles mark the final best-fit *R*-factor after further refinement of the structure (see the text).

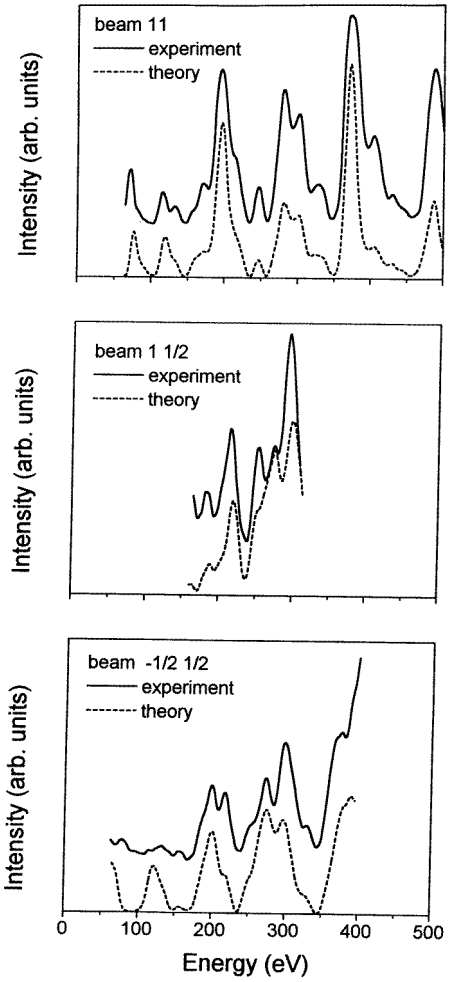

Figure 4. Comparison of the best-fit and experimental spectra for an integer-order, a non-centred, and a centred beam.

the related *R*-factor are still unsatisfactory. As r_{nc} is also slightly higher than expected from mere hydrogen scattering, there must also be some weak substrate reconstruction of (2×2) symmetry which needs to be considered. This can easily be introduced by also displacing those hydrogen-coordinated atoms in the top substrate layer which up to now have remained stationary. They are indicated by light shading in figure 2(c), and belong to the atomic rows in the [001] direction, of which only every second atom is hydrogen coordinated. Again, pulling these atoms out of the surface makes—with simultaneous optimization of all of the other structural parameters—the *R*-factor for the fractional-order beams drop down to $R_f = 0.25$ for *both of the subgroups* of the centred and the non-centred spots. The overall level of calculated intensities for superstructure spots yields $r_t^{calc} = 11.1\%$. In view of the adsorption phase possibly being not fully developed on all crystalline patches of the

substrate, this shows a reasonable agreement with the experimental value $r_t^{exp} = 7.3\%$.

At this point of the analysis, the overall R-factor ($R = 0.16$), as well as the R-factor of the fractional-order beams, $R_f = 0.25$, are low enough to fine tune the hydrogen position. This was done by variation of the adsorption height, and by allowing for horizontal displacements off the ideal threefold-coordinated position towards the long bridge site. Simultaneously, the two top-interlayer distances (measured with respect to the centre-of-mass planes) were optimized, whilst the buckling reconstruction was kept constant. The best fit develops for an adsorbate height of 1.02 Å above the top layer, and a shift of the H atoms towards the long bridge site by 0.05 Å (distance from the long bridge site: $y_H = 0.51$ Å). So, the shift with respect to the former hydrogen site is rather small, rendering another readjustment of the buckling unnecessary. Also, the improvement of the R-factor is marginal (0.002), and consequently this shift is not outside the limits of error (±0.20 Å), as taken from the variance of the Pendry R-factor [25], which amounts to $\mathrm{var}(R) = 0.02$. The structural best-fit results, including error limits for all of the parameters determined, are summarized and discussed in the following section.

Table 1. A compilation of the parameters of the best-fit structure, as determined by means of LEED.

Mo(110)–(2 × 2)H	
y_H (Å)	0.51 ± 0.20
d_H (Å)	1.02 ± 0.20
r_H (Å)	0.57
b_{11} (Å)	0.02 ± 0.01
b_{12} (Å)	-0.04 ± 0.02
$b_1 = b_{11} - b_{12}$ (Å)	0.06 ± 0.01
b_{21} (Å)	-0.015 ± 0.01
b_{22} (Å)	0.015 ± 0.01
$b_2 = b_{22} - b_{21}$ (Å)	0.03 ± 0.01
Δd_{12} (%d_0)	-3.0 ± 0.5
Δd_{23} (%d_0)	0.5 ± 0.7
Δd_{34} (%d_0)	0.0 ± 0.9
d_0 (Å)	2.2236
R_P	0.16
ΔE	3150 eV

4. Results and discussion

The eventually resulting best-fit model is displayed in figure 2(c) in a top view. The line indicates the vertical plane of the section for which the side view is displayed in figure 2(d), including atoms (partly hidden) lying immediately behind the plane of the section. Bold horizontal lines in the side view correspond to the centre-of-mass planes of the layers. The parameters determined are given as well; their numerical values are collected together in table 1. The best-fit Pendry R-factor is $R = 0.16$ ($R_f = 0.25$ for fractional-order beams, $R_i = 0.11$ for integer-order beams). A visual comparison of the experimental and best-fit calculated spectra is provided in figure 4 for a selection of beams, i.e. an integer-order, a centred, and a non-centred beam.

The adsorption structure is characterized by a honeycomb-like arrangement of hydrogen atoms, which reside close to ideally threefold-coordinated sites. They are shifted from the latter by 0.05 ± 0.20 Å towards the long bridge position, from which they have a distance

of $y_H = 0.51 \pm 0.20$ Å. The adsorption height is 1.02 ± 0.20 Å above the centre of mass of the top molybdenum layer. The hydrogen bond length with respect to the two closest coordinated atoms is 1.93 Å, equivalent to a reasonable value of the hydrogen hard-sphere radius, 0.57 Å, which is in the range 0.5–0.6 Å found also for other hydrogen adsorption systems [1]. The relatively large error limits for the adatom position are a result of and consistent with the comparatively weak scattering strength of hydrogen.

It is only by means of a hydrogen-induced substrate reconstruction that the superstructure spot intensities rise to near to the experimentally observed level, and that the structures of the calculated and experimental intensity spectra come close to each other. In the top substrate layer, the reconstruction is characterized by hydrogen-coordinated atoms being pulled out of the surface, leading to a top-layer buckling amplitude of $b_1 = b_{11} - b_{12} = 0.06 \pm 0.01$ Å. Yet not all of the hydrogen-coordinated atoms are lifted by the same amount, as one would suspect at a first glance. Whilst atoms belonging to [001] rows with *all* of their atoms hydrogen coordinated are lifted by 0.06 ± 0.01 Å with respect to uncoordinated atoms, leading to a buckling in the $[\bar{1}10]$ direction, the H-coordinated atoms of neighbouring rows are lifted by only $|b_{12}| = 0.04 \pm 0.02$ Å. This corresponds to an additional buckling within these rows in the [001] direction. These different reconstruction behaviours of H-coordinated atoms may be caused by inequivalences with respect to the adsorbed hydrogen. In fact, this is enhanced by the off-hollow displacement of 0.05 Å obtained for the adatoms. This circumstance seems to corroborate the displacement, which, judging by the LEED analysis alone, is not outside the limits of error.

The reconstruction in the top substrate layer accounts nicely for the intensity levels of the extra spots. If—for a moment—we imagine that all of the atoms reside in the centre-of-mass plane given in figure 2(d), there would be no extra substrate-induced spots. Lifting half of the atoms, i.e. the dark-hatched atoms in figure 2(c), creates two new sublayers which are both of c(2×2) symmetry. Each of them corresponds to 0.5 ML, so they give rise to relatively strong extra centred spots, as observed. By the further displacement of every second atom in the lower sublayer, two sublayers with (2×2) symmetry are created. They contribute to all of the fractional-order spots. With their atomic density of only 0.25 ML and their buckling amplitude smaller than that of the other atoms, the average intensity of non-centred spots is weaker than that of centred spots, again as observed.

There is also a reconstruction in the second molybdenum layer, though it is less pronounced. Atoms more or less directly below the hydrogen atoms (below the darkly hatched atoms in figure 2) are pushed into the surface with respect to the other atoms. This leads to a buckling amplitude of $b_2 = b_{22} - b_{21} = 0.03 \pm 0.01$ Å. The first three interlayer distances (relating to centre-of-mass planes in the case of buckled layers) amount to $d_{12} = 2.156 \pm 0.011$ Å ($\Delta d_{12}/d_0 = -3.0 \pm 0.5\%$), $d_{23} = 2.234 \pm 0.015$ Å ($\Delta d_{23}/d_0 = +0.5 \pm 0.7\%$), and $d_{34} = 2.224 \pm 0.020$ Å ($\Delta d_{34}/d_0 = 0.0 \pm 0.9\%$).

The relaxation obtained at 0.5 ML coverage for the top interlayer distance, $\Delta d_{12}/d_0 = -3.0\%$, lies right in the middle between the values determined for clean and fully hydrogen-covered surfaces, -4.0% and -2.0%, respectively [12]. The next-layer distance is already nearly fully relaxed to the bulk value. Furthermore, the positions of the strongly hatched top-layer atoms, i.e. those which are fully hydrogen coordinated and displaced outward by $b_{11} = 0.02$ Å with respect to the centre-of-mass plane, are practically identical to the positions that these atoms take at full hydrogen coverage [12]. This fits well into the picture in which hydrogen acts locally in such a way as to restore the bonds originally truncated on creation of the surface, and so 'tries' to bring the surface back to a bulk-like-terminated structural state, as observed in many cases [1, 3, 30]. Also, the occupation of

sites of maximum coordination is a feature commonly observed for hydrogen adsorption. It is largely independent of the coverage, as long as the latter allows for and mirrors the dominance of the adatom–substrate interaction over that between adatoms. In addition, surface scientists have become used to the fact that hydrogen in the submonolayer regime induces a buckling of a few hundredths of ångströms at least in the top substrate layer. So, as regards these overall features, the present case of Mo(110)–(2×2)2H turns out to be a rather typical example of a hydrogen adsorption system.

Yet, the details of the reconstruction come as a surprise when comparing the results with those found earlier for Fe(110)–(2×2)2H [9], with the Fe substrate having the same bcc lattice as Mo. Though the magnitude of the atomic displacements is of the same order of magnitude, they are *different in sign* for the atoms of the top substrate layer. Whilst H-coordinated Mo atoms are pulled out of the surface relative to the uncoordinated atoms, the corresponding Fe atoms are pushed into the surface. This is in spite of the fact that, for H/Fe(110), hydrogen also resides near the ideally threefold-coordinated site. Interestingly, it is also slightly displaced from the latter (by 0.14 Å) towards the bridge site, which makes the similarity as regards the atomic environment of hydrogen even closer. Moreover, the hard-core radius resulting from the H–Fe bond length (1.84 Å) is practically the same (0.58 Å). So, the difference in sign of the displacements must be due to the difference between the electronic configurations of Mo and Fe. Probably only exact total energy calculations can provide a deeper and quantitative understanding. This holds also for the shift of hydrogen off the ideally threefold-coordinated site towards the bridge site observed for both H/Mo and H/Fe. Obviously, this shift increases the inequivalence of one of the two H-coordinated substrate atoms to the two others. The inequivalence must be responsible for the difference between the displacement amplitudes of the different atoms, leading to a rather complex buckling reconstruction of the top layer.

With respect to the second substrate layer, the displacement amplitudes of Fe and Mo atoms exhibit the same sign, and the buckling amplitude is almost the same (namely 0.02 ± 0.015 Å for H/Fe [9] versus 0.03 ± 0.01 Å for H/Mo). In view of the different displacements in their top layers, this similarity between Fe and Mo is surprising. It seems to reflect just another feature of the complexity of the electronic rearrangement going on in a substrate upon hydrogen adsorption.

This complexity is also corroborated by the different course of the work-function change $\Delta\varphi$ induced upon hydrogen adsorption on the (110) surfaces of Mo and Fe. For H/Fe(110), there is a nearly continuous work-function decrease with coverage, except for a small break at half-coverage with $\Delta\varphi \approx -55$ meV [14, 15]. The maximum change upon hydrogen saturation is $\Delta\varphi \approx -85$ meV. In the case of H/Mo(110), the work function first decreases to a much deeper minimum ($\Delta\varphi_{max} \approx -320$ meV), and then increases again until, at saturation, $\Delta\varphi \approx +130$ meV [31]. The minimum develops at about the same exposure to hydrogen, where, for H/Fe(110), half-coverage is established. So, it seems that in the early stages of hydrogen adsorption, the work-function change of both surfaces is in the same direction *despite* the difference in sign of the hydrogen-induced top-layer atomic displacements. Even the argument that the work-function decrease arises (at least partly) from the induced corrugation of the surface does not fully hold. For the case of H/Ni(111), an increase of the work function is reported [32], in spite of a hydrogen-induced surface corrugation identical in sign and similar in amplitude to that in the present case of H/Mo(110) [9]. This obviously indicates that the rearrangement of electronic charges upon hydrogen adsorption is rather complex and element specific, so no general predictions can be made without access to precise first-principles calculations.

Acknowledgments

The authors are grateful for financial support through the 'Deutsche Forschungsgemeinschaft' (DFG). MA additionally acknowledges a grant from the 'Studienstiftung des deutschen Volkes' and SS is indebted to the 'Deutscher Akademischer Austauschdienst' (DAAD) for financial support.

References

[1] Heinz K and Hammer L 1996 *Z. Phys. Chem.* **197** 173
[2] Heinz K and Hammer L 1997 *Phys. Status Solidi* a **159** 225
[3] *Surface Structure Database 2.0* 1995 (Gaithersburg, MD: National Institute of Standards and Technology)
[4] Passler M A, Lee B W and Ignatiev A 1985 *Surf. Sci.* **150** 263
[5] Moritz W, Imbihl R, Behm R J, Ertl G and Matsushima T 1985 *J. Chem. Phys.* **83** 1959
[6] Shi M, Bu H, Rabalais J W, Rye R R and Nordlander P 1989 *Phys. Rev.* B **40** 10 163
[7] Hildner M L, Daley R S, Feltner T E and Estrup P J 1991 *J. Vac. Sci. Technol.* A **9** 1604
[8] Schmidt G, Zagel H, Landskron H, Heinz K, Müller K and Pendry J B 1992 *Surf. Sci.* **271** 416
[9] Hammer L, Landskron H, Nichtl-Pecher W, Fricke A, Heinz K and Müller K 1993 *Phys. Rev.* B **47** 15 969
[10] Hassold E, Löffler U, Schmiedl R, Grund M, Hammer L, Heinz K and Müller K 1995 *Surf. Sci.* **326** 93
[11] Hammer L, Kottcke M, Heinz K, Müller K and Zehner D M 1997 *Surf. Rev. Lett.* at press
[12] Arnold M, Sologub S, Hupfauer G, Bayer P, Frie W, Hammer L and Heinz K 1997 *Surf. Rev. Lett.* at press
[13] Hammer L, Arnold M, Heinz K, Kohler B and Scheffler M 1997 *Surf. Sci.* **373** 145
[14] Benzinger J and Madix R J 1980 *Surf. Sci.* **94** 119
[15] Boszo F, Ertl G, Grunze M and Weiss M 1977 *Appl. Surf. Sci.* **1** 103
[16] Altman M, Chung J W, Estrup P J, Kosterlitz J M, Prybyla J, Sahu D and Ying S C 1987 *J. Vac. Sci. Technol.* A **5** 1045
[17] Müller K and Heinz K 1985 *The Structure of Surfaces* ed M A Van Hove and S Y Tong (Berlin: Springer) p 105
[18] Heinz K 1988 *Prog. Surf. Sci.* **27** 239
[19] Heinz K 1995 *Rep. Prog. Phys.* **58** 637
[20] Van Hove M A and Tong S Y 1979 *Surface Crystallography by LEED* (Berlin: Springer)
[21] *American Institute of Physics Handbook* 1972 3rd edn (New York: American Institute of Physics)
[22] Nichtl-Pecher W, Oed W, Landskron H, Heinz K and Müller K 1991 *Vacuum* **41** 297
[23] Pendry J B 1974 *Low Energy Electron Diffraction* (New York: Academic)
[24] Kottcke M, Dötsch B, Hammer L, Heinz K, Müller K and Zehner D M 1997 *Surf. Sci.* **376** 319
[25] Pendry J B 1980 *J. Phys. C: Solid State Phys.* **13** 937
[26] Nichtl-Pecher W, Gossmann J, Hammer L, Heinz K and Müller K 1992 *J. Vac. Sci. Technol.* A **10** 501
[27] Kohler B, Ruggerone P, Wilke S and Scheffler M 1995 *Phys. Rev. Lett.* **74** 1387
[28] Kohler B 1995 *PhD Thesis* Berlin University
[29] Okada M, Baddorf A P and Zehner D M 1997 *Surf. Sci.* **373** 145
[30] Müller K 1993 *Prog. Surf. Sci.* **42** 245
[31] Liu R and Ehrlich G 1982 *Surf. Sci.* **119** 207
[32] Christmann K, Behm R J, Ertl G, Van Hove M A and Weinberg W 1979 *J. Chem. Phys.* **70** 4168